Powder Technology 227 (2012) 3–8

Contents lists available at SciVerse ScienceDirect

Powder Technology

journal homepage: www.elsevier.com/locate/powtec

Fe—Ti oxide nano-adsorbent synthesized by co-precipitation for fluoride removal from drinking water and its adsorption mechanism

Lin Chen, Bo-Yang He, Shuai He, Ting-Jie Wang *, Chao-Li Su, Yong Jin

Department of Chemical Engineering, Tsinghua University, Beijing 100084, China

ARTICLE INFO

Available online 28 November 2011

Keywords:
Fe—Ti oxide
Co-precipitation
Microwave drying
Fluoride adsorption
Hydroxyl group

ABSTRACT

A novel bimetallic oxide adsorbent was synthesized by the co-precipitation of Fe(II) and Ti(IV) sulfate solution using ammonia titration at room temperature. The influences of the washing and drying methods, Fe/Ti molar ratio, and calcination temperature used in the preparation on the morphology, crystallization, surface structure and adsorption capacity were investigated. An optimized Fe—Ti adsorbent had a Langmuir adsorption capacity of 47.0 mg/g, which was much higher than that of either a pure Fe oxide or Ti oxide adsorbent. There was a synergistic interaction between Fe and Ti in which Fe—O—Ti bonds on the adsorbent surface and hydroxyl groups provide the active sites for adsorption, and Fe—O—Ti—F bonds were formed by fluoride adsorption. The novel Fe—Ti adsorbent is efficient and economical for fluoride removal from drinking water.

1. Introduction

Fluoride in minute quantities is an essential component for human health and helps in the normal mineralization of bones and formation of dental enamel, but excessive intake can result in fluorosis. There are more than 20 developed and developing nations where fluorosis is endemic and WHO has given a guideline limitation of less than 1.5 mg/L of fluoride in drinking water [1]. Reverse osmosis, nanofiltration, electrodialysis and Donnan dialysis have been used for fluoride removal [2], but adsorption is considered more efficient for fluoride removal from drinking water because it is simple to operate and cost-effective [2].

Many expensive metal oxide adsorbents with high fluoride adsorption capacities have been developed, such as those using zirconium oxide [3] and rare earth metal oxide [4], but their costs are high. Goethite is a naturally occurring water purifier which is abundant in the earth crust and cheap [5]. Synthetic iron oxide is a good adsorbent for fluoride removal from contaminated water [6–9], but its Langmuir adsorption capacity is low at about 16.5 mg/g [10]. Adsorbents synthesized with iron oxide that incorporate different metal ions for high adsorption performance have been studied. Aluminum (III) [11], zirconium (IV) [12], tin (IV) [13] and chromium (III) [6] ions had been introduced into iron oxide to form bimetallic adsorbents for fluoride adsorption. The synthesis processes and adsorption capacities of these bimetallic oxide adsorbents are summarized in Table 1. It was reported that a new chemical bond formed between the two metal elements through an oxygen atom increased the amount of hydroxyl groups on the adsorbent surface and adsorption capacity of the adsorbents. However, their adsorption capacities were still not high enough and the adsorbents need frequent regeneration.

Recently, a titanium-derived adsorbent was shown to be a potential selective adsorbent for fluoride ions and especially arsenic compounds [14]. Although TiO_2 hardly adsorbs fluoride, it was found that titanium hydroxide ($Ti(OH)_4$) prepared by titrating ammonia into $TiOSO_4$ solution [14,15] or by sol–gel hydrolysis using titanium isopropoxide [16] can exchange fluoride ions. Nanocrystalline titanium dioxide [17], iron (III)-titanium (IV) binary mixed oxide [18] and Ce—Ti [19] oxide adsorbent have been developed to remove arsenate compounds from drinking water. Deng et al. [19] reported that titanium-derived adsorbents produced by hydrolysis at a high temperature had a higher arsenate adsorption capacity than those produced by precipitation at room temperature.

The nano-adsorbent synthesized was of fine powder or a hydroxide floc. It cannot be used directly in a packed bed due to its low hydraulic conductivity and high pressure drop. It needs to be granulated into 1–2 mm granules with a certain strength that can be used directly for adsorption in a packed bed.

In this study, a novel Fe—Ti oxide adsorbent was synthesized by co-precipitation at room temperature. The synergistic interactions between Fe and Ti both during crystallization and fluoride adsorption were investigated. The synthesized adsorbent had a high adsorption capacity and was cost effective. The adsorption mechanism on the Fe—Ti oxide adsorbent was studied.

* Corresponding author. Tel.: +86 10 62788993; fax: +86 10 62772051.
E-mail address: wangtj@tsinghua.edu.cn (T.-J. Wang).

0032-5910/$ – see front matter.
doi:10.1016/j.powtec.2011.11.030

Table 1
Bimetallic oxide adsorbents synthesis and their adsorption capacities reported in the literature.

Adsorbents	Q[a], mg/g	Synthetic method	Structure	Ref.
Fe—Al	17.7	$NH_3 \cdot H_2O$ into $FeCl_3 + AlCl_3$ (1:1)	Crystalline, Fe—O—Al	[11]
Fe—Zr	8.2	NaOH into $FeCl_3 + ZrOCl_2$ (9:1)	Crystalline, Fe—O—Zr	[12]
Fe—Sn	10.5	NaOH into $FeCl_3 + NaSnO_3$	Amorphous, Fe—O—Sn	[13]
Fe—Cr	16.3	$NH_3 \cdot H_2O$ into $FeCl_3 + CrCl_3$ (1:1)	Amorphous, Fe—O—Cr	[6]
Fe—Ti	47.0	$NH_3 \cdot H_2O$ into $FeSO_4 + Ti(SO_4)_2$ (2:1)	Amorphous, Fe—O—Ti	This work

[a] Adsorption capacity by Langmuir isothermal fitting.

2. Experimental

2.1. Materials

$FeSO_4 \cdot 7H_2O$, $Ti(SO_4)_2 \cdot 4H_2O$ and $NH_3 \cdot H_2O$ used were analytical grade (Chemical Engineering Company of Beijing, China). The other chemicals used were also analytical grade reagents.

2.2. Adsorbent preparation

$FeSO_4 \cdot 7H_2O$ and $Ti(SO_4)_2 \cdot 4H_2O$ were dissolved in deionized water to form a mixed solution with total molar concentration of 0.3 M. 12.5% ammonia solution was slowly titrated into the mixed solution under agitation until the pH was 6.9 ± 0.2. The slurry was aged for 48 h. After that, the precipitates were filtrated, washed and dried. The washing was conducted for removing sulfate ions, and used either water or ethanol for washing. The drying was carried out by using either a microwave oven (700 W, 2450 MHz) or a drying oven at 80 °C. The dried product was ground manually to a fine powder and calcined in a furnace. Adsorbents were prepared by different washing and drying methods, Fe/Ti molar ratio and calcination temperature to optimize for a high fluoride adsorption capacity.

2.3. Adsorbent characterization

A high resolution scanning electron microscope (HRSEM, JSM 7401, JEOL Co., Japan) and a high resolution transmission electron microscopy (HRTEM, JEM-2011, JEOL Co., Japan) were used to examine the morphology and micro-structure of the adsorbents. Adsorbent crystallization was studied by X-ray diffraction analysis (D8-Advance, Brucker, Germany) over a range of 10–90° with Cu Kα radiation at a scan speed of 10°/min. The thermal behavior of the adsorbents was analyzed by differential scanning calorimeter and thermogravimetric analysis (TGA/DSC1/16600HT, Mettler-Toledo, Germany). A Fourier transform IR spectrometer (NICOLET 5DX, USA) was used to acquire the IR spectra of the samples. KBr was used to make the samples for FTIR analysis.

The binding energies and atomic ratios of the elements on the adsorbent surface were measured by XPS (PHI Quantera SXM, ULVAC-PHI, Japan). A conventional Al Kα anode radiation source was used as the excitation source. The binding energies were calibrated by the C 1s binding energy at 284.8 eV. XPS data processing and peak fitting were performed using a nonlinear least-squares fitting program (XPSPeak software 4.0, Chemistry, CUHK).

2.4. Adsorption capacity measurement

A fluoride bearing solution was prepared by dissolving NaF in deionized water. 100 mL fluoride solution was added into a conical flask to give an initial fluoride concentration of 50 mg/L. (The high initial fluoride concentration of 50 mg/L used was for easily distinguishing the difference of the adsorption capacity of the adsorbents prepared under different experimental conditions.) 0.1 g adsorbent was added into the flask. The test solution was shaken on a shaker at 150 rpm and kept at 25 °C for 12 h adsorption. After adsorption equilibrium, the adsorbent was separated from the solution by a filter with a 0.22 μm cellulose membrane, and the concentration of residual fluoride in the solution was measured with a fluoride selective electrode connected to an ion meter (PXS-450, Shanghai Kang-Yi Instruments Co., LTD, China). The equilibrium adsorption capacity of the adsorbent was calculated.

3. Results and discussion

3.1. The optimized Fe—Ti adsorbent

Fig. 1 shows a TEM image of the optimized Fe—Ti oxide adsorbent, which was prepared using a Fe/Ti molar ratio of 2:1, ethanol washing, microwave drying, and a calcination temperature of 200 °C. The nanosized structure in the adsorbent was obvious, and the primary particle size was 5–7 nm.

The fluoride adsorption isotherm is depicted in Fig. 2. A saturated fluoride adsorption capacity of 47.0 mg/g was obtained from the fitting of the Langmuir isotherm. It has been reported that the Langmuir adsorption capacities were 17.7 mg/g for a Fe—Al mixed metal oxide [11], 8.2 mg/g for a Fe—Zr hybrid oxide [12], 10.5 mg/g for a Fe—Sn bimetallic oxide [13], and 16.3 mg/g for a Fe—Cr mixed metal oxide

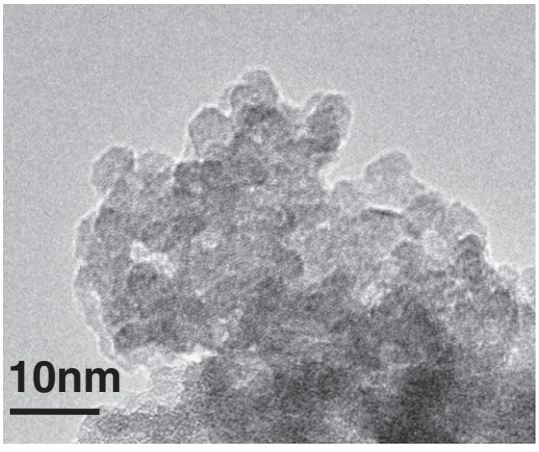

Fig. 1. TEM image of the optimized Fe—Ti oxide adsorbent.

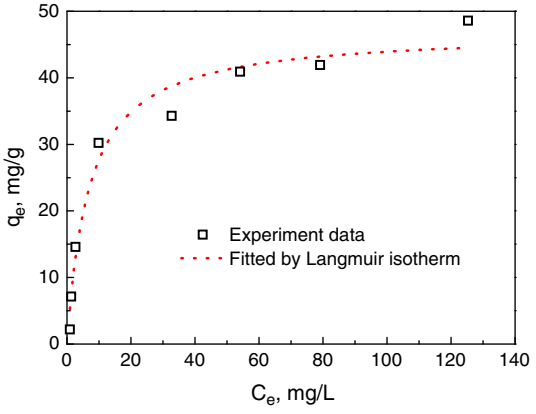

Fig. 2. Adsorption isotherm of the optimized Fe—Ti oxide adsorbent (adsorption dose = 0.5 g/L, adsorption time = 12 h).

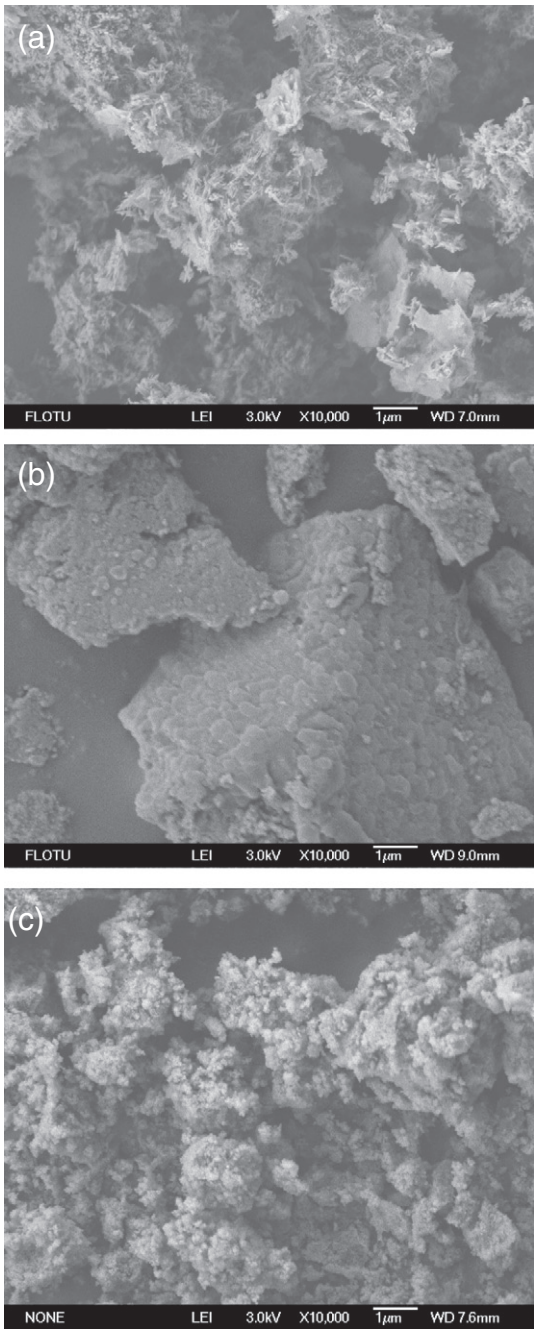

Fig. 3. Surface morphologies of Fe oxide(a), Ti oxide (b), Fe—Ti oxide (c) prepared under the same conditions.

[6]. From the comparison, the 47.0 mg/g capacity of the optimized Fe—Ti oxide was very competitive.

The nano-adsorbent can be granulated or coated onto a carrier into 1–2 mm granules, and then used directly in a packed bed.

3.2. Synergistic interaction between Fe and Ti

For investigating the synergistic interaction between Fe and Ti, a Fe—Ti oxide adsorbent was prepared with a Fe/Ti molar ratio of 1:1 with ethanol washing and microwave drying but without calcination. The equilibrium adsorption capacity of the Fe—Ti oxide adsorbent was 27.09 mg/g at an initial fluoride concentration of 50 mg/L and adsorbent dose of 1 g/L. For comparison, pure Fe oxide and Ti oxide were prepared under the same conditions. The equilibrium

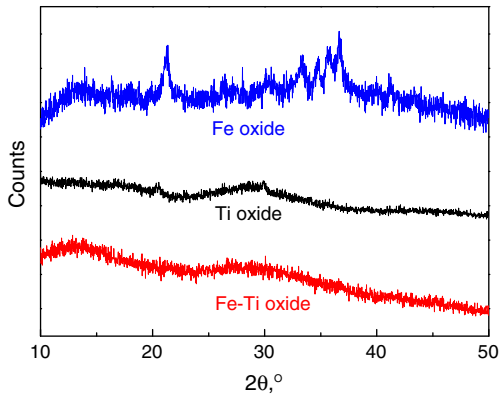

Fig. 4. XRD patterns of Fe oxide, Ti oxide and Fe—Ti oxide adsorbents.

adsorption capacity of Fe oxide was 11.87 mg/g and that of Ti oxide was 8.92 mg/g, which were much lower than that of the Fe—Ti oxide adsorbent of 27.09 mg/g. Furthermore, the equilibrium adsorption capacity of a physical mixture of the Fe oxide and the Ti oxide with an Fe/Ti molar ratio of 1:1 was 17.74 mg/g, which was also lower than that of the Fe—Ti oxide adsorbent.

The morphologies of the Fe oxide, Ti oxide and Fe—Ti oxide prepared under the same condition are shown in Fig. 3. Fig. 3 shows that the shape of the Fe oxide was that of a nano-needle and that of the Ti oxide was that of a nano-sphere, while the shape of the Fe—Ti oxide was that of a much finer nano-sphere. This indicated that the Fe—Ti oxide adsorbent was not a simple mixture of Fe oxide and Ti oxide.

The XRD patterns of the Fe oxide, Ti oxide and Fe—Ti oxide adsorbents are shown in Fig. 4. The spectrum of Fe oxide indicated the presence of crystalline FeOOH. The spectrum of Ti oxide showed the presence of amorphous $Ti(OH)_4$. However, the XRD spectrum of Fe—Ti oxide showed no peaks, which suggested that the co-precipitation process inhibited the formation of the crystalline phase of FeOOH.

The FTIR spectra of the Fe oxide, Ti oxide and Fe—Ti oxide adsorbents are shown in Fig. 5. The bands near 1600 cm^{-1} were assigned to the OH bending vibrational mode of water. The peak at 1401 cm^{-1} was obvious in the spectra of Ti oxide and Fe—Ti oxide but absent in that of Fe oxide. The peaks at 1125 cm^{-1} in the spectra of the three oxides can be assigned to the bending vibration of the hydroxyl of metal oxides (M-OH). It was found that the peaks at 1401 and 1125 cm^{-1} can be considered as the fingerprints for the active sites of the adsorbents from the discussed below. The peak at 587.9 cm^{-1} was assigned as the characteristic peak of Fe oxide, and that at 615.2 cm^{-1} to be that of Ti oxide. However, the Fe—Ti oxide adsorbent had its characteristic peak at a lower wave number of

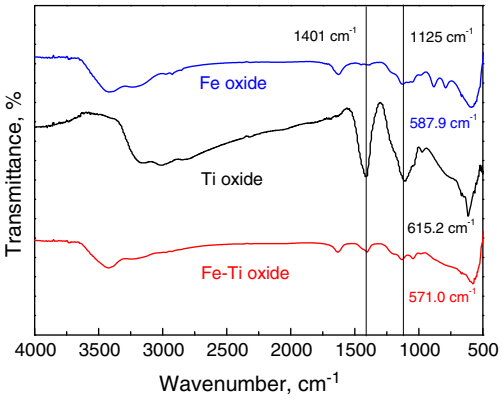

Fig. 5. FTIR spectra of Fe oxide, Ti oxide and Fe—Ti oxide adsorbents.

Table 2
Effect of washing and drying methods on the adsorption capacity of Fe—Ti oxide adsorbents (adsorption dose = 1 g/L, initial fluoride concentration = 50 mg/L, adsorption time = 12 h).

Washing	Drying	Additional	Adsorption capacity, mg/g
Water	Dry oven		6.49
Water	Microwave(MW)		7.63
Ethanol	Dry oven		11.07
Ethanol	Dry oven	MW heating	10.72
Ethanol	Microwave		27.09

571.0 cm^{-1}, which was clearly lower than those of Fe oxide and Ti oxide. From this blue shift, it was inferred that Fe—O—Ti bonds were formed in the bimetallic Fe—Ti oxide adsorbent.

From the above analysis of the adsorption capacities, morphologies, and XRD and FTIR spectra of the adsorbents, it can be inferred that the Fe—Ti oxide adsorbent was not a simple mixture of Ti oxide and Fe oxide, and that a synergistic interaction between Fe and Ti occurred during the synthesis.

3.3. Optimization of the Fe—Ti oxide adsorbent preparation

3.3.1. Effect of washing and drying methods

For optimizing the preparation condition of the Fe—Ti oxide adsorbent, a Fe—Ti oxide precipitate was prepared by co-precipitation with a Fe/Ti molar ratio of 1:1 and then treated with different washing and drying methods. It was found that the washing and drying methods for the precipitate had a remarkable effect on the adsorption capacity of the adsorbents. The data are shown in Table 2. When ethanol washing and microwave drying were both employed, the adsorption capacity of the adsorbent was increased significantly to 27.09 mg/g.

Ethanol is known to be a better dispersant than water in the drying process, and it can restrict particle agglomeration due to the condensation of hydroxyl groups [20]. Microwave drying provides rapid heating and activation of the hydroxyl groups on the particle surface, especially for high BET surface nano-adsorbents [21,22]. It is probable that the combination of ethanol washing and microwave drying resulted in a high surface area and plentiful activated hydroxyl groups, which increased the adsorption capacity.

The weight loss of the adsorbents due to different washing and drying methods were analyzed. The data are shown in Fig. 6. The weight loss of the Fe—Ti adsorbent synthesized with ethanol washing and microwave drying was much higher than those synthesized using other washing and drying methods, which indicated that the amount of surface hydroxyl groups on it was much more. Table 2 and Fig. 6 show that a large weight loss corresponded to a large amount of hydroxyl groups on the adsorbent surface, and high adsorption capacity. Thereafter, ethanol washing and microwave drying were used in the optimized adsorbent preparation.

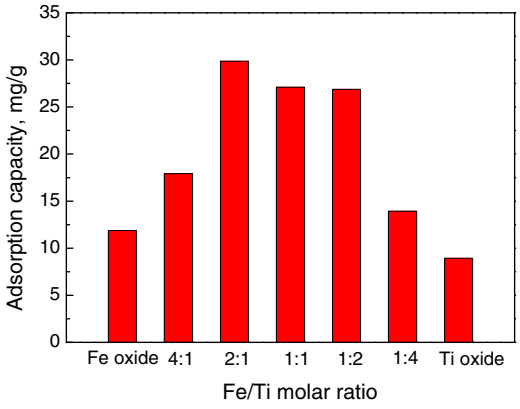

Fig. 7. Effect of Fe/Ti molar ratio on fluoride adsorption capacity of the Fe—Ti oxide adsorbents (adsorption dose = 1 g/L, initial fluoride concentration = 50 mg/L, adsorption time = 12 h).

3.3.2. Effect of the Fe/Ti molar ratio

The effect of the Fe/Ti molar ratio on the adsorption capacity is shown in Fig. 7. The Fe—Ti adsorbent reached the highest adsorption capacity of 29.85 mg/g, which was much higher than that of the pure Fe oxide and Ti oxide adsorbents, at the Fe/Ti ratio of 2:1. This showed the remarkable synergistic effect of Fe and Ti on fluoride adsorption capacity. Therefore, the Fe/Ti molar ratio of 2:1 was used in the optimized adsorbent preparation.

3.3.3. Effect of calcination temperature

The adsorption capacities of the Fe—Ti oxide adsorbents calcined at 200, 400, 600, and 800 °C were measured and shown in Table 3. The highest adsorption capacity was achieved when the adsorbent was calcined at 200 °C. The adsorption capacity decreased to 3.61 mg/g when the adsorbent was calcined at 800 °C.

Table 3
Adsorption capacity of Fe—Ti oxide adsorbents calcined at different temperatures (adsorption dose = 1 g/L, initial fluoride concentration = 50 mg/L, adsorption time = 12 h).

Temperature, °C	none	200	400	600	800
Adsorption capacity, mg/g	29.85	31.24	24.10	15.03	3.61

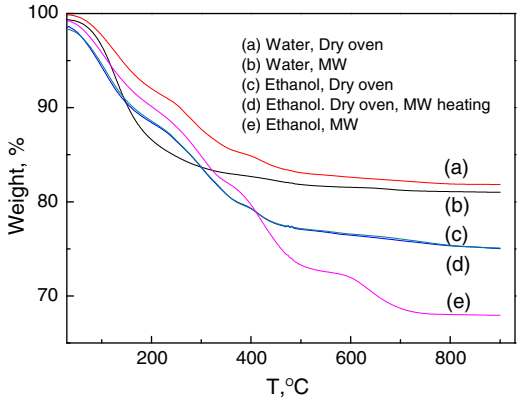

Fig. 6. TG curves of Fe—Ti oxide adsorbents treated by different washing and drying methods (MW = microwave drying).

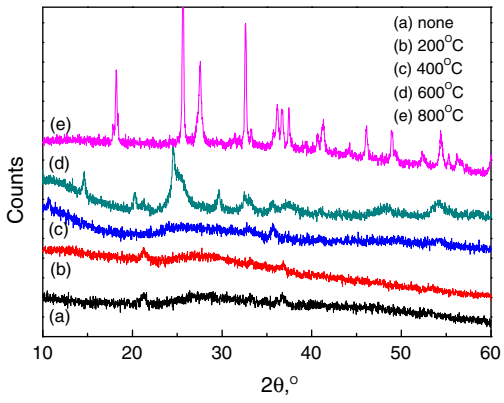

Fig. 8. XRD patterns of Fe—Ti oxide adsorbents produced using different calcination temperatures (Fe/Ti molar ratio 2:1).

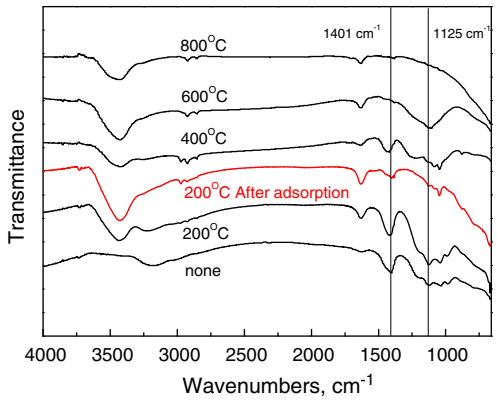

Fig. 9. The FTIR spectra of Fe—Ti oxide adsorbents produced using different calcination temperatures and the optimized Fe—Ti adsorbent after fluoride adsorption (Fe/Ti molar ratio 2:1).

The XRD patterns of the Fe—Ti oxide adsorbents calcined at the different temperatures are shown in Fig. 8. When the calcination temperature was lower than 400 °C, the Fe—Ti adsorbent retained its amorphous structure. When the temperature was higher than 600 °C, the spectra of the adsorbent showed crystalline peaks, which suggested that an amorphous structure was associated with a high adsorption capacity. Wu et al. [2] have reported that the change away from the amorphous structure of a Fe—Al—Ce trimetal oxide adsorbent at high calcination temperature caused a decreased adsorption capacity for fluoride.

The FTIR spectra of the adsorbents calcined at the different temperatures are shown in Fig. 9. The intensity of the peaks at 1401 and 1125 cm^{-1} increased when 200 °C was used but decreased when the calcination temperature was increased to 400 °C. It was inferred that surface hydroxyl groups were partially removed at high temperatures. Therefore, the calcination temperature at 200 °C was used in the optimized adsorbent preparation.

3.4. Adsorption mechanism on the Fe—Ti adsorbent

The FTIR spectra in Fig. 9 showed that the intensity of the characteristic peak of the optimized adsorbent at 1401 and 1125 cm^{-1} decreased after adsorption. This further verified the involvement of surface hydroxyl groups in fluoride adsorption [23].

To further explore the adsorption mechanism of fluoride on the Fe—Ti adsorbent surface, the adsorbents were analyzed by XPS before and after adsorption [24–26]. The relative amounts (%) in terms of the atoms of Ti, Fe, O and F in different adsorbents are summarized in Table 4. The atomic fraction of F in the surface layer of the adsorbent increased from 0% to 6.51% after adsorption, which indicated that fluoride ions had been adsorbed. Fig. 10 shows the O 1s spectra of the optimized Fe—Ti oxide adsorbent before and after adsorption. The O 1s spectra can be divided into two peaks, namely, one at 529.0 eV assigned to O^{2-} (bonding with metal) and another at 530.5 eV assigned to OH^- (hydroxyl) groups on the surface. The spectra were fitted using a 50:50 Gaussian:Lorentzian peak shape, and showed that the hydroxyl groups on the adsorbent surface

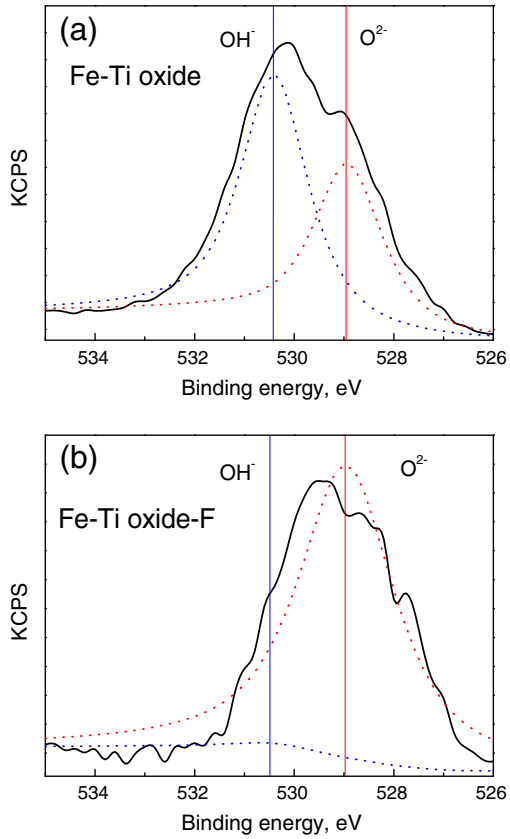

Fig. 10. XPS spectra of the O 1s of the optimized Fe—Ti adsorbents and the fitted distribution of O^{2-} and OH^- (a) before adsorption; (b)after fluoride adsorption.

decreased remarkably after adsorption. The details are listed in Table 5. After fluoride adsorption, the relative area ratio for the peak at 530.5 eV attributed to OH^- decreased from 58% to 1.3%, while the relative area ratio of O^{2-} increased from 42% to 98.7%. This suggested that hydroxyl groups on the adsorbent surface played an important role in fluoride adsorption, which is consistent with the FTIR analysis.

Fig. 11 shows the XPS spectra of the Ti 2p peak of Ti oxide and the optimized Fe—Ti adsorbent before and after fluoride adsorption. The binding energy of the Ti 2p peak was increased from 456.2 to 456.8 eV when Ti oxide was co-precipitated with Fe oxide. Since the electronegativity of Fe (1.83) is higher than Ti (1.54), when Ti was bonded to Fe through O, the Ti—O shielding was weakened, which would explain the increase of the Ti 2p binding energy. After adsorption, the binding energy of the Ti 2p peak increased from 456.8 eV to 457.2 eV. It was inferred that a Fe—O—Ti—F bond was formed. Since the electronegativity of F (3.98) is the highest among the elements, the presence of F led to a weakening of O—Ti shielding, causing the Ti 2p binding energy to increase by 0.4 eV. Therefore, the Fe—O—Ti bond in the Fe—Ti bimetallic adsorbent supported the active site (Fe—O—Ti—OH) for fluoride adsorption by forming a Fe—O—Ti—F bond on the adsorbent surface.

Table 4
Atomic ratios from XPS data of the optimized Fe—Ti adsorbents before and after fluoride adsorption.

Atomic ratios, %	Ti	Fe	O	F
Fe—Ti oxide	13.38	6.33	80.30	0
Fe—Ti oxide-F	18.43	6.47	68.58	6.51

Table 5
Distribution of O^{2-} and OH^- from fitted XPS spectra of the O 1s peak of the optimized Fe—Ti adsorbents before and after fluoride adsorption.

Sample	Peak	B.E. , eV	FWHM, eV	Percent, %
Fe—Ti oxide	O^{2-}	528.92	1.68	42
	OH^-	530.4	1.6	58
Fe—Ti oxide-F	O^{2-}	528.95	2.28	98.7
	OH^-	530.4	1.7	1.3

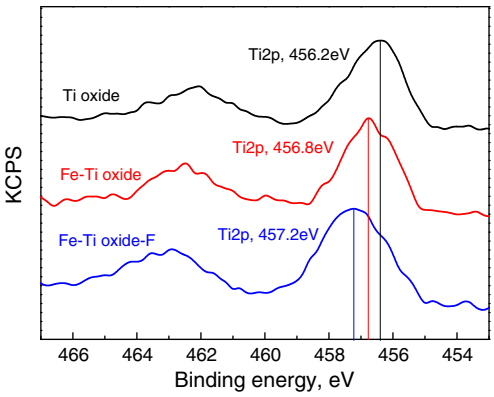

Fig. 11. XPS spectra of the Ti 2p of Ti oxide and the optimized Fe—Ti adsorbents before adsorption and after adsorption.

4. Conclusion

A novel Fe—Ti bimetallic oxide adsorbent was synthesized by the co-precipitation of Fe(II) and Ti(IV) sulfate solution using ammonia titration at room temperature. An optimized adsorbent, which was synthesized with a Fe/Ti molar ratio of 2:1, ethanol washed, microwave dried and calcined at 200 °C, had a Langmuir adsorption capacity of 47.0 mg/g. Fe and Ti in the Fe—Ti oxide adsorbent interacted synergistically to give increased fluoride adsorption capacity. The hydroxyl groups and Fe—O—Ti bonds on the adsorbent surface provided the active sites for adsorption, and formed a Fe—O—Ti—F bond after fluoride adsorption. The novel Fe—Ti adsorbent is efficient and economical for fluoride removal from drinking water.

Acknowledgements

The authors wish to express their appreciation of financial support of this study by the National Natural Science Foundation of China (NSFC No. 20906055 and No. 21176134).

References

[1] Meenakshi, R.C. Maheshwari, Fluoride in drinking water and its removal, Journal of Hazardous Materials 137 (1) (2006) 456–463.
[2] X. Wu, Y. Zhang, X. Dou, M. Yang, Fluoride removal performance of a novel Fe—Al—Ce trimetal oxide adsorbent, Chemosphere 69 (11) (2007) 1758–1764.
[3] X.P. Liao, B. Shi, Adsorption of fluoride on zirconium (IV)-impregnated collagen fiber, Environmental Science and Technology 39 (12) (2005) 4628–4632.
[4] A.M. Raichur, M.J. Basu, Adsorption of fluoride onto mixed rare earth oxides, Separation and Purification Technology 24 (1–2) (2001) 121–127.
[5] Y.L. Tang, J.M. Wang, N.Y. Gao, Characteristics and model studies for fluoride and arsenic adsorption on goethite, Journal of Environmental Sciences (China) 22 (11) (2010) 1689–1694.
[6] K. Biswas, S. Debnath, U.C. Ghosh, Physicochemical aspects on fluoride adsorption for removal from water by synthetic hydrous iron(III)-chromium(III) mixed oxide, Separation Science and Technology 45 (4) (2010) 472–485.
[7] M. Streat, K. Hellgardt, N. Newton, Hydrous ferric oxide as an adsorbent in water treatment—part 1: preparation and physical characterization, Process Safety and Environment 86 (B1) (2008) 1–9.
[8] M. Streat, K. Hellgardt, N. Newton, Hydrous ferric oxide as an adsorbent in water treatment—part 2: adsorption studies, Process Safety and Environment 86 (B1) (2008) 11–20.
[9] M. Streat, K. Hellgardt, N. Newton, et al., Hydrous ferric oxide as an adsorbent in water treatment—part 3: batch and mini-column adsorption of arsenic, phosphorus, fluorine and cadmium ions, Process Safety and Environment B1 (2008) 21–30.
[10] S. Dey, S. Goswami, U.C. Ghosh, Hydrous ferric oxide (HFO)—a scavenger for fluoride from contaminated water, Water, Air, & Soil Pollution 158 (1) (2004) 311–323.
[11] K. Biswas, S.K. Saha, U.C. Ghosh, Adsorption of fluoride from aqueous solution by a synthetic iron(III)–aluminum(III) mixed oxide, Industrial and Engineering Chemistry Research 46 (16) (2007) 5346–5356.
[12] K. Biswas, D. Bandhoyapadhyay, U.C. Ghosh, Adsorption kinetics of fluoride on iron(III)–zirconium(IV) hybrid oxide, Adsorption 13 (1) (2007) 83–94.
[13] K. Biswas, K. Gupta, U.C. Ghosh, Adsorption of fluoride by hydrous iron(III)–tin(IV) bimetal mixed oxide from the aqueous solutions, Chemical Engineering Journal 149 (1–3) (2009) 196–206.
[14] T. Wajima, Y. Umeta, S. Narita, K. Sugawara, Adsorption behavior of fluoride ions using a titanium hydroxide-derived adsorbent, Desalination 249 (1) (2009) 323–330.
[15] T. Ishihara, Y. Shuto, S. Ueshima, H.L. Ngee, H. Nishiguchi, Y. Takita, Titanium hydroxide as a new inorganic fluoride ion exchanger, Journal of the Ceramic Society of Japan 110 (9) (2002) 801–803.
[16] L.N. Ho, T. Ishihara, S. Ueshima, H. Nishiguchi, Y. Takita, Removal of fluoride from water through ion exchange by mesoporous ti oxohydroxide, Journal of Colloid and Interface Science 272 (2) (2004) 399–403.
[17] M. Pena, X.G. Meng, G.P. Korfiatis, C.Y. Jing, Adsorption mechanism of arsenic on nanocrystalline titanium dioxide, Environmental Science and Technology 40 (4) (2006) 1257–1262.
[18] K. Gupta, U.C. Ghosh, Arsenic removal using hydrous nanostructure iron(III)–titanium(IV) binary mixed oxide from aqueous solution, Journal of Hazardous Materials 161 (2–3) (2009) 884–892.
[19] S.B. Deng, Z.J. Li, J. Huang, G. Yu, Preparation, characterization and application of a Ce–Ti oxide adsorbent for enhanced removal of arsenate from water, Journal of Hazardous Materials 179 (1–3) (2010) 1014–1021.
[20] J.Y. Wu, The research of the controlled preparation and the craft on the TiO_2, nanoparticle (2004) M. Diss. Xiangtan Univ.
[21] A.F. Shojaie, M.H. Loghmani, La^{3+} and Zr^{4+} co-doped anatase nano TiO_2 by sol-microwave method, Chemical Engineering Journal 157 (1) (2010) 263–269.
[22] J.N. Hart, Y.B. Cheng, G.P. Simon, L. Spiccia, Challenges of producing TiO_2 films by microwave heating, Surface and Coatings Technology 198 (1–3) (2005) 20–23.
[23] Y. Zhang, M. Yang, X. Huang, Arsenic(V) removal with a Ce(IV)-doped iron oxide adsorbent, Chemosphere 51 (9) (2003) 945–952.
[24] Y. Zhang, X.M. Dou, M. Yang, H. He, C.Y. Jing, Z.Y. Wu, Removal of arsenate from water by using a Fe—Ce oxide adsorbent: effects of coexistent fluoride and phosphate, Journal of Hazardous Materials 179 (1–3) (2010) 208–214.
[25] Y. Zhang, M. Yang, X. Dou, H. He, D. Wang, Arsenate adsorption on a Fe—Ce bimetal oxide adsorbent: role of surface properties, Environmental Science and Technology 39 (18) (2005) 7244–7251.
[26] S.B. Deng, H. Liu, W. Zhou, J. Huang, G. Yu, Mn-Ce oxide as a high-capacity adsorbent for fluoride removal from water, Journal of Hazardous Materials 186 (2–3) (2011) 1360–1366.